Mon. Not. R. astr. Soc. (1987) **225,** 531–550

Surface photometry of powerful radio galaxies – II. Relations with the radio, optical, and clustering properties

S. J. Lilly* *Princeton University Observatory, Peyton Hall, Princeton, New Jersey 08544, USA*

R. M. Prestage *Steward Observatory, University of Arizona, Tucson, Arizona 85721, USA*

Accepted 1986 October 21. Received 1986 October 21; in original form 1986 July 29

Summary. CCD images of a sample of 31 powerful radio galaxies with $z<0.25$ in the southern hemisphere have been obtained to measure their magnitudes and values of the structure parameter α and to record the incidence of multiple nuclei. These data have been compared with similar data for bright galaxies in Abel clusters and have been related, within the sample, to a variety of other properties of the radio galaxies, particularly the structure of the extended radio lobes, the strength of nuclear emission lines and the richness of the cluster environment. Radio galaxies with FR I structure and/or weak emission lines are similar to first-ranked Abell cluster galaxies, while the more powerful radio galaxies with FR II structure and stronger emission lines have lower optical luminosities. The underlying galaxies in the broad-line radio galaxies that have substantial unresolved nuclear components are also of generally lower optical luminosity. The total absolute magnitudes of the radio galaxies are correlated with the cluster density (measured on scales of order 1 Mpc) in the same way as has been found for the generally much richer Abell systems, and a common formation process may be operating. The incidence of multiple nuclei is a strong function of environment, with no radio galaxies in poor clusters having secondary nuclei that cannot be easily ascribed to a chance projection. The dumb-bell optical morphology is strongly associated with 'head–tail' radio structure, and two examples of dumb-bell galaxies undergoing unusual interaction have been found.

1 Introduction

Over the past few years there has been growing interest in the part played in the active galactic nucleus (AGN) phenomenon by the host galaxies and their immediate cluster environments. Some of this work was recently reviewed by Balick & Heckman (1982). Many of these

*Present address: Institute for Astronomy, University of Hawaii, 2680 Woodlawn Drive, Honolulu, Hawaii 96822, USA.

investigations have concentrated on relatively nearby low-luminosity AGNs and have sought to determine what causes the onset of nuclear activity. Such studies have often highlighted individual peculiarities of the host galaxies. Other studies have been directed at more powerful sources, such as the radio sources in the well-known 3CR catalogue, and are aimed at determining what conditions are necessary for an AGN to attain an exceptional luminosity. These studies have frequently been statistical in nature and have concentrated on the overall trends seen in well-defined samples of sources. The question of the production of radio sources of exceptional luminosity may be particularly relevant in seeking to understand the evolution with cosmological epoch that is seen in the radio source population, since it is believed that it is the more powerful sources that are primarily responsible for this evolution (see e.g. Longair 1966; Peacock 1985).

As part of this work on powerful radio sources, Lilly, McLean & Longair (1984, hereafter LML) studied the optical surface brightness profiles of a sample of 10 3C radio galaxies in the redshift interval $0.03<z<0.3$ that were identified with luminous 'classical double' radio sources. To facilitate comparison with the samples of Abell cluster galaxies studied by Hoessel (1980) and Schneider, Gunn & Hoessel (1983), these data on the 3C radio galaxies were parameterized by the metric absolute magnitude $M_{V,\gamma}$ and the structural parameter α_γ first introduced by Gunn & Oke (1975). This latter parameter measures the logarithmic slope of the growth curve at a sampling radius γ taken to be $19.2\,h^{-1}$ kpc (where $H_0=50h$ km s^{-1} Mpc^{-1}) and is discussed in more detail by LML. The location of the 3C radio galaxies on the M_V, α plane was compared with that of the first-ranked Abell cluster galaxies and a number of conclusions reached. Principal amongst these was the fact that these powerful radio galaxies were generally of somewhat lower optical luminosity (i.e. lower M_V and smaller α) than typical first-ranked Abell cluster galaxies, a conclusion that had implications for some recent investigations into the properties of radio galaxies at high redshift. Unfortunately, the small number of radio galaxies involved in that initial study, and their rather uniform radio properties, rendered it impossible to investigate the relationship between (M_V, α) and other properties of the radio galaxies, such as the radio structure and luminosity, the strength of optical emission lines, and so on. Despite this limitation, a number of suggestions were made on the basis of earlier qualitative work (e.g. Matthews, Morgan & Schmidt 1964).

To study these possible relationships in more detail, we have undertaken the present systematic study of a much larger complete sample of powerful radio galaxies in the southern hemisphere. The definition of the sample is such that numerous examples of sources with radio luminosities both above and below $P(2.7\,\mathrm{GHz})$ about $10^{24.5}$ W Hz^{-1} sr^{-1} are included in the sample. This luminosity is at the break in the radio luminosity function and is associated with the appearance of classical double radio structure. It also marks the point above which the differential evolution of the radio source population is strongest, and may be generally thought of as representing a lower bound to the luminosities of the 'most powerful' radio sources. Examples of both Fanaroff–Riley Class I and Class II sources (Fanaroff & Riley 1974, FR) are included in the sample. In optical terms, the sample contains some broad-line radio galaxies (BLRG), a BL Lac object, and numerous narrow-line radio galaxies (NLRG) in which the strength of the emission lines ranges from strong through weak to apparently absent.

This range of properties in the sample enables us to investigate the relationships between the host galaxy, its cluster environment, and the manifestations of extreme nuclear radio activity. Our principal motivation has been to discover what factors are responsible for determining whether a radio source will be able to attain the highest luminosities $P(2.7\,\mathrm{GHz})$ $\geqslant 10^{24.5}$ W Hz^{-1} sr^{-1}.

The layout of the paper is as follows. In the next section the selection criteria for the sample are listed, the observations and their reduction described, and the analysis to yield the photometric parameters presented. In Section 3 the principal observational results are presented and

discussed. The implications of these results on ideas about radio galaxies and the general AGN phenomenon are discussed in Section 4. Finally, in Section 5 we summarize our conclusions. A value of $H_0=50\,\mathrm{km\,s^{-1}\,Mpc^{-1}}$ is used throughout the remainder of the paper, and the subscript γ is implied on all M_V and α, with the value of γ taken as 19.2 kpc.

2 Data

2.1 THE SAMPLE OF RADIO GALAXIES

Thirty-five radio galaxies were observed in this programme. These were selected from three well-defined subsamples of the 2.7-GHz 2-Jy all-sky statistical sample of Wall & Peacock (1985, WP). All of these were bounded by the right ascension range accessible in December, 22^h–14^h.

The first statistical subsample constructed from the WP catalogue consists of all radio galaxies with declination $+10°\geqslant\delta\geqslant-45°$ and redshift $0.010\leqslant z\leqslant0.100$. Nineteen of 20 radio galaxies in this sample were observed, mostly in both B and R, and this is the sample that is most complete (the only source omitted, 0404+03, was done so inadvertently). The declination limits were chosen so that both high-quality VLA radio maps (Prestage *et al.*, in preparation) and UK Schmidt optical plates for clustering studies (Prestage & Peacock, in preparation) were potentially available for these sources.

The second subsample consisted of a higher redshift extension of the first, $0.100\leqslant z\leqslant0.25$. All eight radio galaxies in this subsample were observed, but unfortunately four of them do not have a spectroscopically determined redshift. These galaxies could not be used in the analysis and are not considered further in this paper. This subsample is therefore not as complete as the first, although the omission of those radio galaxies that lack a spectroscopic redshift is not thought to introduce a significant bias to this group. It should be pointed out that the four galaxies excluded in this way have photometrically estimated redshifts (on the basis of their apparent magnitudes and the typical absolute magnitudes of similar radio galaxies) that are sufficiently large (0.15, 0.18, 0.20 and 0.20) that it is unlikely that they actually have redshifts such that they should be members of the first subsample defined to have $z\leqslant0.10$.

Finally, eight radio galaxies with $0.01\leqslant z\leqslant0.10$ lying outside the declination limits of the first sample were also observed, and hence these fields lack either the high-resolution VLA radio maps or the wide-field optical plates. Their inclusion was random, and no biases should be introduced by their inclusion in our analysis.

For most purposes we have considered all 31 radio galaxies to belong to a single sample and are confident that our conclusions are not affected by this. The above selection criteria should nevertheless be borne in mind if the data are to be used for other purposes.

2.2 DATA ACQUISITION AND REDUCTION

The observations were made on the nights of 1983 December 9–11 using the 3.9-m Anglo–Australian Telescope (AAT) and the Royal Greenwich Observatory (RGO) camera at prime focus employing an RCA 512×320 CCD detector. Weather conditions during the run were very variable, with widely varying transmission and seeing. Nevertheless, the more distant galaxies in the sample were only observed during periods of the best seeing (~1 arcsec) and at least one photometric exposure was obtained of each galaxy. All the galaxies were observed through a Cousins R filter, and many were also observed with a B filter approximating the photographic J band. Photometric calibration of the CCD images was obtained using defocused images of six standard stars from Graham (1982), with $13<V<15$, and of four brighter stars from Landolt (1983). These were used to define a colour equation relating the instrumental magnitudes to the standard photometric systems.

The usual dark-current and bias exposures were taken through the run. The bias offset, which did show some structure, was found to remain constant, and an average bias frame was constructed from all of the bias exposures and subtracted from each astronomical image. The dark current was shown to be negligible. Flat-field exposures were taken at the start and end of each night by pointing the telescope at a white area on the inside of the dome that had been illuminated by a tungsten lamp. For each set of flat-fields a number of exposures were made of varying length and intensity of illumination. These were found to be satisfactorily linear. There appeared to be only very small variations in the flat-fields determined at the start and end of each night, so an average of these was taken and this flat-field applied to the astronomical exposures. This procedure resulted in very flat images for all except a very small number of exposures taken either during twilight or very close to the Moon. After flat-fielding, the R images clearly suffered from the addition of a fringe pattern caused by thin-film interference of emission lines in the night sky. These were satisfactorily removed using interactively determined multiples of a 'fringe-frame' kindly provided by Dr Bill Pence, then of the AAO.

The reduced images were photometrically calibrated through the computation of the instrumental offset for B and R. Airmass corrections of 0.24 and 0.10 mag per airmass for B and R, respectively (Gilmore & Pence, private communication), were applied to the standard star and radio galaxy images.

Small corrections were applied to the observed magnitudes to remove the effects of Galactic extinction. The reddening maps by Burstein & Heiles (1982) were used for this purpose, assuming $A(B)=3.5\,E(B-V)$ and $A(R)=2.0\,E(B-V)$. In only a very few cases was $E(B-V)>0.1$, and it was generally less than 0.55.

2.3 DATA ANALYSIS

As in LML our main analysis of the radio galaxy images concentrates on the derivation of the metric magnitude measured through an aperture of 19.2 kpc, M_V, and the structure parameter α at that radius. Our reasons for this choice should be discussed.

First, these two parameters are easily derived observable quantities. They are relatively stable to the effects of seeing and hence of redshift. Indeed they can probably be estimated to $z\sim1$ even from the ground in good seeing conditions and are hence useful in comparisons between samples at high and low redshift. Secondly, the simple definition of α, in terms of the mean surface brightness and the mean enclosed surface brightness at the sampling radius of 19.2 kpc, makes the effect of various perturbations on the basic galaxy profile easy to visualize. This is particularly the case for the addition of an unresolved nuclear component, a situation of obvious relevance in the present investigation. Thirdly, a large body of data on the brighter members of Abell clusters has been published in this form, and comparisons are thus facilitated by the use of these parameters. Finally, the standard photometric parameters such as effective radius or total luminosity can in any case be fairly easily derived once the necessary assumptions as to the form of the surface brightness profile have been made. M_V and α are therefore believed to be well suited to this statistical investigation.

The derivation of these parameters followed closely the procedures described by LML. For each galaxy, the local sky brightness was determined by computing the median pixel value found in an annulus of radii 58 and 77 kpc (i.e. between 3 and 4γ) and subtracted from the image. The centre of each radio galaxy was found by determining the centroid of the central 5-arcsec area of the radio galaxy image. Contaminating stars and other galaxies were removed from the images using the algorithms described by LML. This process included the removal of the few 'multiple nuclei' found in the radio galaxies; in this context, we use 'multiple nucleus' to refer to secondary maxima in the surface brightness distributions which have an integrated luminosity substantially

less than that of the main body of the galaxy, and which produce asymmetric isophotes in the radio galaxy only in the neighbourhood of the secondary peak. The five radio galaxies that were clearly 'double' in the sense that they were composed of two components of approximately equal luminosities were treated separately, since in these cases it is not possible to isolate a single underlying galaxy. These galaxies, which we will henceforth refer to as 'dumb-bells', are further discussed in Section 3.5.

Our reasons for removing the secondary nuclei are as follows. First, there is some doubt in the case of first-ranked Abell cluster galaxies as to whether these so-called nuclei are truly associated with the main galaxy or whether they are simply chance superpositions, (see e.g. Merritt 1984; Hoessel, Borne & Schneider 1985). Secondly, the presence of two or more maxima in the two-dimensional surface brightness distribution can clearly affect the α parameter measurement, or indeed, any other profile-fitting algorithm. The effect on α can be of either sign, depending on whether the secondary component is enclosed or bisected by the 19.2-kpc sampling radius, and this may introduce considerable scatter into the measurements for the sample. In view of the size of the sample and of our desire to have as meaningful measurements as possible, we therefore decided to remove these secondary components, noting their presence when doing so. Our analysis differs in this respect from those of Hoessel (1980) and of Schneider *et al.* (1983). Since the incidence of multiple nuclei is much lower in this sample than in the Abell cluster samples studied by them (see Section 3.4), this procedural difference is unlikely to seriously affect any comparisons between the radio galaxy and Abell cluster samples.

Aperture magnitudes centred on the nucleus of the radio galaxy were computed for successively larger closely spaced radii. A low-order polynomial was then fitted in the vicinity of 19.2 kpc to the integral growth curve of the logarithm of the enclosed luminosity versus the logarithm of the radius. From this, the value and slope of the curve at that point, and hence directly the metric magnitude and α, were calculated. The blue and red images were analysed identically. As in LML, the uncertainties in the magnitudes are believed to be about 0.05 mag, and those in α to be about 5 per cent.

The five dumb-bell galaxies (0123−01, 0255+05, 0428−53, 0625−53 and 1251−129 could not be analysed in this way, since it was not possible to define a meaningful centre about which to measure the aperture magnitudes. So, following Hoessel (1980) and Schneider *et al.* (1983), the centre of these systems was defined to be the centre of that 19.2-kpc radius aperture that maximized the enclosed light, and then M_V and α were determined in the usual way. Because of its very low redshift (0.015) and the slight off-centring of the galaxy on our CCD image, it turned out that this procedure could not be reliably carried out in the case of 1251−12. The parameters for the remaining four galaxies are listed in Table 1 in parentheses.

The atmospheric seeing in each image was determined from a simple one-parameter Gaussian fit to the small number of stars visible on each exposure. Since they are determined at the relatively large radius of 19.2 kpc, equivalent to 7 arcsec at $z\sim0.1$ and over 1 arcmin at $z\sim0.01$, neither M nor α is very sensitive to the seeing. LML discussed the effect of seeing on α and showed that the correction to the observed value was small as long as the seeing Gaussian σ was $<0.2\gamma$ (their fig. 2). Although the seeing FWHM varied between 1 and 4 arcsec on our run, our policy of matching the redshift of the galaxies observed at a given time to the prevalent seeing conditions ensured that for 75 per cent of our observations σ/γ was less than 0.1, and for all of them it was less than 0.2. A small correction was therefore applied to the observed values of α according to the curves in fig. 2 of LML.

The fully corrected R-magnitudes, $(B-R)$ colours, and $\alpha(B)$ and $\alpha(R)$ measurements are listed in Table 1. The R apparent magnitudes were used to calculate a metric absolute V-magnitude in a $a_0=0.5$ cosmology, using the K-corrections of Pence (1976) and a rest-frame $(V-R)$ colour of 0.60. This transformation to $M(V)$ was primarily made for historical reasons and will not be

Table 1. Data.

id	z	R	(B-R)	α(B)	α(R)	M_V	n	B_{gg}*	FR	HL
0034-01	0.073	15.03	1.52	0.39	0.41	-22.81	0	21	I	B
0043-42	0.053	15.56	1.54	0.40	0.39	-21.54	1	17	IIg	B?
0055-01	0.045	13.70	1.45	0.50	0.54	-23.04	0	102	I	B
0123-01	0.018	(11.27)	(1.47)	(0.53)	(0.56)	(-23.44)	1	101	TT	B
0131-36	0.030	12.77	-	-	0.55	-23.08	0	47	IIn	B
0255+05	0.024	(12.41)	(1.44)	(0.40)	(0.45)	(-22.93)	1	225	TT	B
0305+03	0.029	12.20	1.44	0.51	0.54	-23.56	0	42	I	B
0325+02	0.030	13.52	1.39	0.66	0.64	-22.32	0	51	IIn	B
0349-27	0.066	15.58	1.14	0.79	0.62	-22.03	0	33	IId	A
0430+05	0.033	13.04	0.90	0.18	0.23	-23.01	0	-29	U	BLRG
0453-20	0.035	13.19	1.36	0.64	0.63	-22.99	0	164	I	B
0521-36	0.062	14.18	1.11	0.17	0.22	-23.29	0	38	I	BLLac
0625-35	0.055	13.93	1.42	0.50	0.56	-23.27	1	N/A	I	B
0915-11	0.065	14.14	1.37	0.78	0.85	-23.44	1	160	I	B
0945+07	0.086	15.72	1.24	0.27	0.28	-22.50	0	14	IIg	BLRG
1251-12	0.015	-	-	-	-	-	1	103	TT	B
1318-43	0.011	10.68	-	-	0.59	-22.95	0	N/A	I	B?
1333-33	0.013	10.35	-	-	0.55	-23.64	0	N/A	I	B
2221-02	0.056	14.95	1.65	0.20	0.20	-22.29	0	-5	IId	BLRG
0035-02	0.220	17.80	-	-	0.38	-22.72	0	85	I	A
0038+09	0.188	18.50	-	-	0.43	-21.61	0	N/A	IId	A
2211-17	0.153	16.86	-	-	0.85	-22.74	1	105	IIn	B
2314+03	0.220	17.25	-	-	0.24	-23.27	0	N/A	IId	BLRG
0106+13	0.060	14.95	-	-	0.44	-22.44	0	210	IIg	A
0356+10	0.031	14.07	-	-	0.32	-21.84	0	14	IId	A
0428-53	0.039	(12.82)	-	-	(0.62)	(-23.60)	2	440	I	B
0518-45	0.035	14.71	1.14	0.28	0.29	-21.47	0	49	IId	A
0620-52	0.051	13.41	-	-	0.77	-23.60	2	N/A	I?	B
0625-53	0.054	(13.29)	-	-	(1.18)	(-23.86)	2	N/A	1?	B
0802+24	0.060	15.10	1.36	0.36	0.35	-22.30	0	48	IId	A
2356-61	0.096	15.65	1.47	0.57	0.59	-22.83	0	N/A	IId	A

correct for galaxies such as the BLRG, which have significant non-thermal components and non-stellar colours. It does, however, facilitate comparisons with other workers. The values of M_V so derived are also tabulated in Table 1; the values for the four dumb-bells are listed in parentheses.

2.4 OTHER DATA

As mentioned in Section 2.1, the radio galaxies observed here form a complete subsample of the all-sky catalogue of Wall & Peacock (1985), and a growing amount of other data are available for them.

All the extended sources with declinations between +10° and −45° have recently been mapped with the C-configuration VLA (Prestage *et al.*, in preparation). Cambridge 5-km synthesis maps have been published for the three most northerly sources, 0106+13, 0356+10 and 0802+24 (Jenkins, Pooley & Riley 1977; Laing 1981); for the four most southerly sources there are low-resolution Fleurs synthesis maps for 0428−53 and 2356−61 (Christiansen *et al.* 1977) but not for 0620−52 or 0625−53. Data on these last two sources from the Molongolo telescope suggest that, while they are both extended, neither of them has prominent double structure (Large *et al.*

1981; Hunstead 1972). These various radio data have been used to classify each source morphologically according to the scheme of Fanaroff & Riley (1974). The further classification of the 'quality' (good, doubtful, not) of the 'classical doubleness' as defined by Longair & Riley (1979) has been determined for the FR II sources. The two sources for which only very low-quality structure information is available (0620−52 and 0625−53) have both been classified as 'FR I?'. These classifications are given in Table 1. FR I sources with 'twin-tail' structure are noted as 'TT', while the unresolved source is indicated by a 'U'.

Unfortunately, the optical spectroscopic data available for these sources are much less homogeneous than the radio data described above. Nevertheless, some data have been taken for almost all of the sources. Many of the galaxies have been studied by Osterbrock and collaborators or by Danziger and collaborators. Drs Gilmore and Fosbury have kindly given us access to a considerable amount of unpublished data, while data on the remaining sources are scattered through the literature (Costero & Osterbrock 1977; Danziger, Fosbury & Penston 1977; Danziger *et al.* 1979; Danziger *et al.*1984; Danziger & Goss 1983; Goss *et al.* 1980; Koski 1978; Osterbrock, Koski & Phillips 1976; Phillips & Osterbrock 1975; Smith, Spinrad & Smith 1976; Tritton 1972; Whiteoak 1972; Yee & Oke 1978). The inhomogeneity of these data makes it impractical to use a quantitative measure of the strength of the emission lines, and so we have adopted the qualitative classification scheme of Hine & Longair (1979, henceforth HL). Class A sources have strong lines, while Class B sources have lines that are weak or absent. These 'A' and 'B' classifications are listed in Table 1 for the NLRG. The BLRG, which are all HL Class A sources, have been indicated as 'BLRG'. Only for two sources is the classification in some doubt. No data have been found for 1318−43 (the redshift is a 1975 private communication to Schilizzi) and for 0043−42 only the old photographic redshift reference is available. Both these sources have been classified as Class B, since the presence of strong emission lines would probably have been remarked upon. The source 0518−45 (Pictor A) shows evidence for broad emission lines. This unusual source has been discussed by Danziger *et al.* (1977), and it is possible that much of the emission is not photoionized by a non-stellar active nucleus. We have nevertheless treated this as a standard BLRG in our discussion.

The cluster environments of a large fraction of the sample have recently been studied by Prestage & Peacock (in preparation). Following the analysis by Longair & Seldner (1979), the density or richness of the environment is parameterized by B_{gg*}, which is the amplitude of the three-dimensional spatial cross-correlation function of galaxies about the radio galaxy position. This is determined using galaxy counts to a certain limiting magnitude to construct the two-dimensional angular correlation function, and a knowledge of the radio galaxy redshift and of the general galaxy luminosity function. In principle, B_{gg*} should be directly proportional to the number of galaxies that lie within 1 Mpc of the radio galaxy. This method corrects in a statistical way for the contamination produced by unrelated foreground objects. Values of B_{gg*} are listed in Table 1 for those galaxies for which the parameter has been determined. In most cases, the galaxy counts in the neighbourhood of the radio galaxy were carried out using COSMOS measures of UK Schmidt Survey Plates; otherwise the Lick counts were used (see Prestage & Peacock for a full discussion). Those sources that do not have B_{gg*} values in Table 1 are those for which a UK Schmidt Survey Plate was not available for measurement by the COSMOS machine, and their exclusion is therefore entirely unrelated to their astrophysical properties.

3 Presentation of results

In this section we present our observational results derived from the data described in the previous section. In Section 3.1 we briefly discuss the colour data and the differences in the α measurements made in B and R. In Section 3.2 we examine the locations on the (M_V,α) plane of

the radio galaxies as functions of their other properties, and explore the relationships between them and also between the radio galaxies and other giant ellipticals found in Abell clusters. In Section 3.3 we analyse the radio galaxies as a function of their cluster environment, again making reference to the properties of Abell cluster galaxies. In Section 3.4 we discuss the incidence of multiple nuclei as a function of radio morphology and cluster environment, and in Section 3.5, we briefly discuss the five dumb-bell galaxies.

3.1 THE $(B-R)$ COLOURS

The metric $(B-R)$ colours from Table 1 are plotted in Fig. 1 as a function of redshift for the 17 radio galaxies in our sample for which they were measured. The BLRG and the BL Lac object are represented as crosses, the remainder as solid points. The solid line represents the colours of ordinary giant ellipticals. This line has a zero-point of 1.36, derived from the colour equations of Bessell (1979) and Blair & Gilmore (1982), and the $(B-V)=0.98$ and $(B-R)=0.86$ colours of nearby giant elliptical galaxies (Sandage 1973), and a slope of $2.2z$ taken from the K-corrections of Bruzual (1981).

All the solid points follow the gE curve well. The scatter in the data can be explained as a combination of the effect of a colour–magnitude relation and the dispersion in absolute magnitude, and observational uncertainties. The starred points lie off from this line, which represents the colour of redshifted starlight. Three of the BLRGs (including the peculiar Pictor A) and the BL Lac object are bluer, while one of the BLRGs is redder. This is presumably due to the presence of a non-stellar radiation component in these galaxies that is probably associated with the active nucleus. In four cases this has a shallower spectral index than the starlight, leading to a blue-excess for the galaxy, while in the other the non-stellar component is redder.

This may be further investigated by studying the measurements of α made at B and R. For the twelve 'normal' radio galaxies on Fig. 1 (i.e. excluding the BLRGs and the BL Lac object) the mean difference between $\alpha(b)$ and $\alpha(R)$ is -0.02, i.e. the blue images are generally very slightly more compact. The scatter in this quantity is 0.03, reflecting the uncertainty in measuring the α parameter, which for our data is probably rather greater at the shorter wavelengths due to the decreased flux densities from the galaxies and the lower sensitivity of the CCD detector.

In Fig. 2, the ratio $\alpha(B)/\alpha(R)$ has been plotted for all 17 radio galaxies as a function of the rest-frame $(B-R)$ colour, corrected from the observed colours using the colour K-correction of $2.2z$. The 12 normal radio galaxies lie in a clump in this diagram with $\alpha(B)\sim\alpha(R)$ and

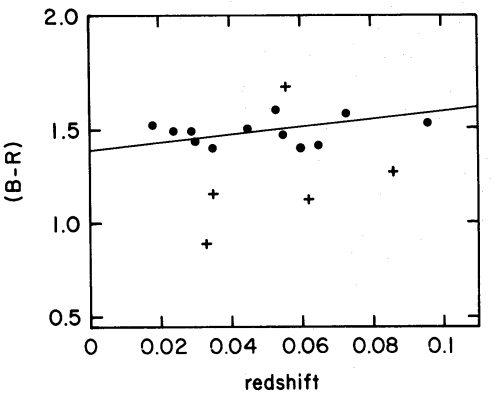

Figure 1. The observed $(B-R)$ colour as a function of redshift for those radio galaxies observed in both bands. BLRGs and the one BL Lac are plotted as crosses, the remainder as solid circles. The solid line represents the colour of a normal giant elliptical.

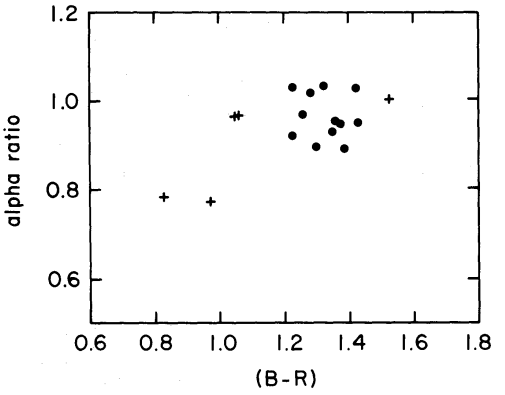

Figure 2. The rest-frame $(B-R)$ colour for the galaxies shown in Fig. 1 plotted as a function of the ratio of $\alpha(B)/\alpha(R)$.

$(B-R)\sim1.36$, while the five objects that would be expected to have sizeable non-stellar components lie away from this clump. On the assumption that α is independent of wavelength for the underlying stellar component, the location of an object on the diagram should in principle indicate the spatial distribution of the additional non-stellar component. For instance, adding any unresolved nuclear component to a normal radio galaxy with $\alpha(B)=\alpha(R)$ and $(B-R)=1.36$ would move the galaxy to the lower left in Fig. 2, the precise location being determined by the strength and effective spectral index of the additional component.

Those galaxies that might be expected to contain a non-stellar nuclear component lie away from the remainder and are located in the general direction expected from a simple model for such a component. The data for the remaining galaxies give no reason to believe that they contain non-stellar components sufficiently large to affect the measurements of M_V and α.

3.2 THE (M_V, α) DIAGRAM

As a preliminary to our discussion of the (M_V,α) diagram for the radio galaxies we refer to Fig. 3(a). On this diagram, we have plotted the locations on the (M_V,α) plane of the first-, second- and third-ranked galaxies in the 79 Abell clusters observed by Schneider *et al.* (1983). These parameters have been derived from the values of R_e and the Reduced Absolute Magnitude (RAM) tabulated by them. Their location on the diagram can be taken as indicating the locus of non-radio giant elliptical galaxies.

We have also indicated on this diagram two lines that are relevant to our future discussion. First, we have plotted the curve that is produced by the addition of an unresolved nuclear component to an otherwise normal galaxy, since from the previous section this is clearly appropriate to the cases of the BLRG and the BL Lac object. It is trivial, from the definition of α in terms of the ratio of the surface brightness at the sampling radius to the mean surface brightness interior to it, to show that, as an unresolved component is added, the value of α will decrease as the metric brightness increases: $d\alpha/\alpha=0.94\times dM$. For a given BLRG with a non-stellar nucleus, therefore, the properties of the underlying galaxy are in principle constrained to lie somewhere on the curve that passes through the point representing that particular BLRG or BL Lac object.

Secondly, since it is possible, by assuming a de Vaucouleurs profile, to derive a total magnitude from M_V and α, we have plotted on the figure the locus of points with the same total magnitude M_{tot}. This curve is important, because it represents the effect of viewing a non-spherical galaxy from different orientations, and because it offers a convenient and relatively meaningful way to project the galaxies on to a single curve in the figure. Both of these curves may be shifted in the vertical direction.

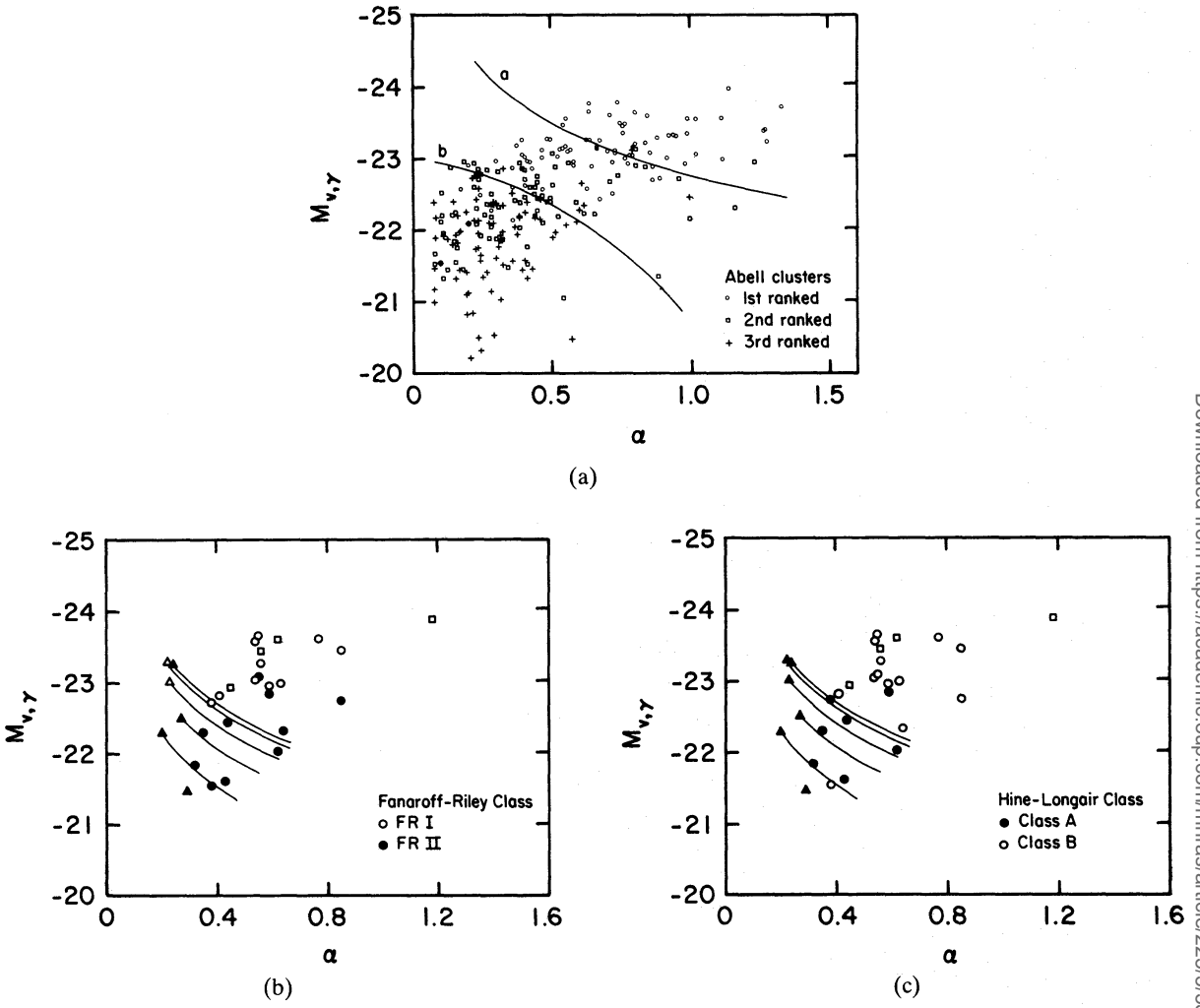

Figure 3(a). The (M_V, α) diagram for first- (circles), second- (squares) and third-(crosses) ranked members of Abell clusters observed by Schneider *et al.* (1983). The upper line indicates the effect of adding an unresolved nuclear component to a galaxy, and the lower line is the locus of constant total absolute magnitude assuming a de Vaucouleurs profile. (b). The (M_V, α) diagram for radio galaxies. BLRGs are presented by triangles, dumb-bells by squares and normal radio galaxies by circles. FR II sources (powerful classical doubles) are represented by solid symbols, other radio types by open symbols. The lines emanating from each BLRG represent decompositions into an underlying galaxy plus an unresolved component terminated at an arbitrary point. (c). As in (a), except that Hine & Longair Class A sources (strong emission lines) are shown filled and Class B sources (weak or absent lines) are shown open.

The (M_V,α) diagram for the radio galaxies, produced from the R metric magnitudes and direct measurements of α, is presented in Figs. 3(b) and (c), in which the following conventions have been used: the BLRG and the BL Lac object are indicated by triangles, the dumb-bell galaxies, whose parameters are determined in a way that is slightly different from the other galaxies, by squares, and the 'ordinary' radio galaxies by circles. In the two diagrams, these symbols representing the radio galaxies are either filled or open, depending on some additional parameter in each diagram, namely the Fanaroff–Riley classification of the radio morphology in Fig. 3(b), and the Hine–Longair classification of the strength of the optical emission lines in Fig. 3(c).

On the two diagrams, we have also indicated the track followed by each of the five BLRG and the BL Lac object as progressive amounts of an unresolved nuclear component are removed using the curve shown in Fig. 3(a).

On Fig. 3(b), we have differentiated the radio galaxies on the basis of their radio morphology. Radio sources with Fanaroff–Riley Class II structure are represented by filled circles. The FR II radio structure has brightness maxima that are located towards the outer extremities of the lobes. These FR II sources therefore exhibit a range of morphologies from the most classical of the 'classical doubles', which are dominated by intense hotspots at the outer extremities of the symmetric lobes, to those with less well-developed hotspots and more asymmetric structures. All the other sources, including FR Class I 'woofly double' sources, 'twin-tail' sources and the single unresolved source are represented by open symbols. All these sources have surface brightness maxima that peak near to the centre of the source, but again, a wide range of structures are inevitably included in this category. Nevertheless, despite this diversity within each FR classification, it is clear that this differentiation produces a remarkably good segregation in the diagram, with the FR II sources being associated with galaxies with fainter M and smaller α than the remainder. It is difficult to quantify this since the FR classification scheme is only two-valued. Nevertheless, we note that the single FR II galaxy with $\alpha \sim 0.85$ (2211−17) is the least well-developed FR II in the sample and was very nearly classified as an FR I (see Section 2.4 for a radio map reference for this and all other sources). Indeed, when the 'quality' of the 'classical double' (based on the symmetry of the source and the prominence and location of the hotspots; see Longair & Riley 1979 and Table 1) is introduced on to Fig. 3(b), it is found that the 'best' ones lie furthest from the FR Is, with those near to the FR I area generally being 'poorer' examples with less symmetric sources and less prominent hotspots.

It should be noted that the addition of a non-stellar nuclear component to a galaxy moves it in a direction orthogonal to the displacement seen between the two different classes of radio morphology, and hence this cannot be responsible for the difference. Similarly, a rotation of even a highly triaxial body cannot account for it and so orientation effects can be ruled out. Indeed, we can think of no mechanism that will cause a galaxy to move from that area of the diagram occupied by the FR II sources into that occupied by the remainder and then back again. The inescapable conclusion is that the host galaxies of FR II sources are generally different from those of FR I and other sources and that consequently these two radio morphologies cannot represent different evolutionary states of a given source, as might once have been imagined.

We note in passing that such a division may even be apparent in the galaxies with substantial non-stellar components. The underlying galaxies of those that have FR II structure appear, from the decomposition curves in Fig. 3(b), to lie generally below the two that do not have this radio structure.

Comparison with the distribution of Abell cluster galaxies in Fig. 3(a) shows that the non-FR II sources have optical structures very similar to those found in the first-ranked Abell clusters studied by Schneider *et al.* (1983), while the FR II sources are more similar optically to the second- or third-ranked galaxies. This will be discussed later in connection with the cluster environments of these galaxies.

In Fig. 3(c) we have replotted the radio galaxy data, this time differentiating between those that have strong emission lines, whether broad or narrow (HL Spectral Class A), which are represented as solid points, and those in which the emission lines are either weak or absent i.e. HL Class B, which are represented as open symbols. Since it is known (e.g. Hine & Longair 1979) that there is a relation between the strength of the emission lines and the FR Class of the galaxy, it is not surprising that a similar separation between HL Class A and B objects is seen in Fig. 3(c) as was evident in Fig. 3(b).

The decomposition curves of the galaxies with substantial non-stellar radiation components are especially interesting in this context. The underlying galaxies clearly originate from the area occupied by the strong-lined narrow-line radio galaxies, which are represented by the solid circles, rather than from the area occupied by the weak-lined objects, the open circles in Fig. 3(c).

It is conceivable that a selection effect is operating in Fig 3(c), since, in contrast to Fig. 3(b), the distinguishing classification of class A or Class B, and NLRG or BLRG has been made on the basis of optical criteria. One could imagine that a given nucleus, whether broad-lined or narrow-lined, will be more readily visible in a lower luminosity galaxy, i.e. one in the lower left of Fig. 3(c). The central surface brightnesses of the galaxies of different luminosities should not vary very much, however, and so we are confident that the differentiation seen in Fig. 3(c) is real.

In summary, these data strongly indicate that some property, or properties, that manifest itself/themselves at least in part in the optical luminosity [i.e. the location in the (M_V, α) plane] is responsible for determining both the radio structure and luminosity, and the strength of the nuclear emission lines. Since the galaxies associated with FR II radio structure and strong emission lines cannot transform themselves into those associated with FR I radio structures and weaker emission lines, it follows that these different radio structures and emission-line strengths cannot represent different phases in the life of a given active nucleus. In addition, the data show that the conditions which allow the presence of strong lines and FR II structure also allow the presence of broad lines and substantial non-stellar components, generally not found in the other galaxies.

A similar conclusion has been hinted at before. Longair & Seldner (1979) showed FR I and FR II sources to have different cluster environments that also cannot change significantly with time. That analysis was, however, based on a statistical analysis of the Lick galaxy counts, with a statistical correction for foreground contamination highly dependent on redshift (and hence FR Class), whereas our analysis is based on a very direct study of the properties of the host galaxies, which should be quite independent of redshift. This difference between FR I and FR II sources was also suggested by LML, who compared their observations of 10 strong-lined FR II sources from the 3C catalogue with the very early qualitative descriptions of the appearance of low-luminosity radio galaxies (with predominantly FR I radio structure) that appeared in Matthews *et al.* (1964), and implied high luminosities and values of the α parameter. The present analysis has confirmed this initial suggestion that the host galaxies of FR I and FR II sources would be distinguishable in a statistical sense.

3.3 THE ABSOLUTE MAGNITUDE AS A FUNCTION OF CLUSTER ENVIRONMENT

In this section we discuss the relationship between the photometric properties of the galaxies and their cluster environments. Because of the complex form of the (M_V, α) diagram and the curvature of the correlation between these two parameters, we have chosen to combine them into a total magnitude when investigating the relationships between the photometric properties of the galaxies and their cluster environments. If a de Vaucouleurs' $r^{1/4}$ surface brightness distribution is assumed, then there is a simple relationship between the metric magnitude and α and the total magnitude $M_{\rm tot}$. A line of constant $M_{\rm tot}$ was plotted in Fig. 3(a), and it may be seen that this is approximately orthogonal to the M_V–α correlation at all α. $M_{\rm tot}$ therefore represents a convenient parameter for describing the location of a galaxy on the diagram. The total magnitude obviously has some physical meaning, but it should be emphasized that these values have not been directly measured from the data and will not be strictly correct for any galaxy that does not follow an $r^{1/4}$ surface brightness distribution. In an attempt to minimize the likelihood of this, the dumb-bell galaxies, which clearly do not have an $r^{1/4}$ distribution were treated separately. These total magnitudes were estimated by summing the total enclosed light within a large radius (about 55 kpc). For all of the remaining normal (i.e. non-BLRG) radio galaxies, the total magnitude was computed using the observed values of the metric magnitude and α.

There is an important additional reason for choosing $M_{\rm tot}$ as the photometric parameter. It can be seen that the two curves in Fig. 3(a), representing a line of constant $M_{\rm tot}$ and the effect of

decomposing an N-galaxy into a galactic and an unresolved component, are approximately parallel for $0.3<\alpha<0.6$, which is the likely range of α of the underlying galaxy [see Fig. 3(b) and (c). Hence the total magnitude of the underlying galaxy in the five BLRGs and the BL Lac object can be estimated fairly well from the simple measurements of the metric magnitude and α, despite not knowing the precise degree of contamination from the nucleus, and hence the exact location of the underlying galaxy along the decomposition curves in Fig. 3(b) and (c). Taking reasonable values from the decomposition curve, we have done this for each of the six galaxies that may have a significant unresolved component.

For a statistic describing the cluster environment, we have used the parameter B_{gg^*} mentioned in Section 2.4. As discussed earlier, this is defined in terms of the amplitude of the cross-correlation function of galaxies, but, for the present purposes, it may be regarded simply as a parameter that is proportional to the total number of galaxies within 1 Mpc of the object in question, in this case the radio galaxy, normalized to the mean density of galaxies in the Universe. Because galaxies are clustered, the mean value of B_{gg^*} averaged over all galaxies is equal to about 40; hence $B_{gg^*}/40$ should be the ratio of the number of galaxies within 1 Mpc of the particular object, as opposed to the number that would have been expected around a galaxy chosen at random. Values of $B_{gg^*}<-1.0$ are unphysical. Unfortunately, the procedure for determining B_{gg^*} involves the statistical deprojection of the observed two-dimensional distribution of neighbour galaxies on the sky, and this can introduce sufficient scatter to make $B_{gg^*}<-1.0$.

We have plotted the total absolute magnitude, M_{tot}, and B_{gg^*} for the radio galaxies in Fig. 4. The cluster parameter, B_{gg^*}, is plotted on a logarithmic scale, and the two galaxies (both BLRGs) that have the unphysically negative values of B_{gg^*} have been arbitrarily assigned values of +8, and these points are enclosed by brackets in Fig. 4.

There is clearly a well-defined relationship between the total magnitude of the radio galaxy and the number of galaxies located within 1 Mpc of it. This relation includes the normal radio galaxies, the underlying galaxies of those with substantial non-stellar radiation components, and the dumb-bell galaxies.

Schneider *et al.* (1983) have shown that a similar relation exists for the members of Abell clusters. Using the values of r_e and RAM given by Schneider *et al.* (1983) we have computed the total magnitudes of the first-, second- and third-ranked members in their 83 clusters. These total magnitudes have been binned by the Abell Richness Class, and for each of these we have shown in

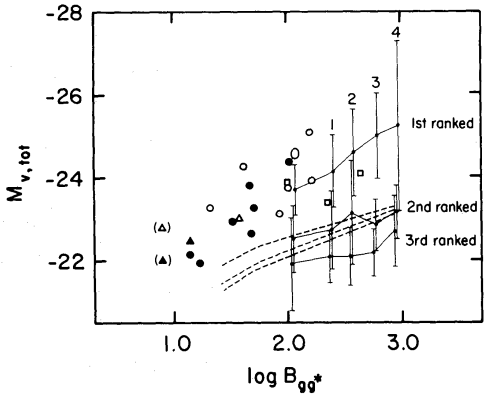

Figure 4. The variation of total absolute magnitude with cluster parameter B_{gg^*}. Symbols are as in Fig. 3(b) (differentiation by FR class). The three sets of five connected points with error bars represent the total absolute magnitudes of the first- second- and third-brightest galaxies for five Abell Richness Classes from Schneider *et al.* (1983). Inner tick marks indicate the uncertainty in the mean; outer bars represent the dispersion in each class. The three dashed lines are estimates of the expected absolute magnitudes for the first three galaxies if they are drawn from a Schechter function.

Fig. 4 the mean M_{tot}, the uncertainty in the mean (inner tick marks) and the 1σ dispersion in the sample (outer tick marks). The Abell Richness Classes have been assigned values of B_{gg^*} in the following way: from the Abell cluster sample of Leir & van den Bergh (1977), 11 Richness 0 clusters with accurate redshifts are found to have a mean value of 112 ± 12, 15 Richness 1 clusters have a mean value of 272 ± 28, and 13 Richness 2 clusters have a mean value of 388 ± 48. We have adopted these values for these Richness Classes, extrapolating to richer classes using the simple definition of Richness Class in terms of the number of members of such clusters. For some of the multiple objects in the Abell cluster sample of Schneider *et al.* (1983), i.e. those that have multiple nuclei or consist of superposed galaxies, which patently do not have $r^{1/4}$ surface brightness distributions, the estimate of the total magnitude may be in error. In the cases of the second- and third-ranked galaxies, the problem is not important, because less than 7 per cent of the sample are not simple isolated systems (Schneider *et al.* 1983), but for the first-ranked galaxies, about 40 per cent of which have been so contaminated, it is more severe. Rejection of all such multiple systems does not alter the second- and third-ranked curves significantly and only affects the richest two bins of the first-ranked galaxies, reducing the means by 0.5 and 1.0 mag, respectively. In view of the large dispersion in these last two bins, we have nevertheless decided to include the multiple systems, for completeness, in computing the points in Fig. 4.

The magnitude–richness relation for the powerful radio sources is clearly contiguous with that of the first-ranked Abell cluster galaxies and separate from that of the second- or third-ranked galaxies. In other words, the radio galaxies appear to be very similar to the central galaxies in Abell clusters, albeit in somewhat poorer environments and of rather lower total optical luminosities.

Assuming $M^* \sim -21.8$ and $\alpha=1.25$ (Felten 1977), we have also sketched on the diagram the expected magnitudes of the first-, second-, and third-brightest galaxies as a function of Richness Class taken from Schechter (1976). Some recent determinations of the luminosity function (e.g. Kirschner, Oemler & Schechter 1979) have suggested that the value of M^* should be revised brightwards by $\sim$0.5 mag (see e.g. Felten 1985), which would result in a similar displacement of the curves on the diagram. Even with this uncertainty, however, it is clear that the first-ranked Abell cluster galaxies and the radio galaxies lie substantially above the expected relation. This former fact has been known for some time and has contributed to the acceptance of the idea that some special formation mechanism may be responsible for the appearance of the brightest galaxy. The present work indicates that this process has probably also operated in the cases of the radio galaxies, which lie in areas of considerably lower average galactic density (measured on the scale of $\sim$1 Mpc) than the centres of Abell clusters.

We note in passing the good agreement of the predicted and observed magnitudes of the second-ranked galaxies but the apparent discrepancy in the case of the third-ranked galaxies. We believe that this may represent an effect of the relatively small sampling area used by Schneider *et al.* (1983) in selecting the second- and third-brightest galaxies in the cluster, and suspect that a galaxy brighter than the listed third-ranked might be found further from the cluster centre.

Our interpretation of Fig. 4 is that it indicates that the powerful radio galaxies are qualitatively rather similar to first-ranked galaxies in Abell clusters except that they are found in much sparser cluster environments. In particular, if the high luminosities of the first-ranked Abell galaxies are due to some special formation or evolutionary process, then it is likely that this has also acted on the radio galaxies.

3.4 THE INCIDENCE OF MULTIPLE NUCLEI AND OF NEARBY COMPANIONS

In view of both the high fraction of first-ranked Abell cluster galaxies that have multiple nuclei (Hoessel 1980; Schneider *et al.* 1983) and the many recent suggestions that nuclear activity is

stimulated by encounters with neighbouring galaxies, it is of interest to examine the frequency of multiple nuclei and of nearby galaxies in this well-defined sample of radio galaxies.

For each image, the number of secondary maxima within a projected radius of 19.2 kpc, which we call multiple nuclei, and the number of galaxies whose projected distances from the radio galaxy nucleus were between 19.2 and 50 kpc were determined. It is estimated that a secondary nucleus would have been detected if its integrated luminosity was within 3–4 mag of the integrated luminosity of the dominant galaxy. This rather small outer radius was chosen so that all but the nearest radio galaxies could be treated in exactly the same way, this region being visible on the CCD images for all $z>0.015$. The number of secondary nuclei in each radio galaxy is listed in Table 1.

The identification of the multiple nuclei may clearly depend on several factors including their luminosities, the seeing conditions and the redshift of the galaxy. Because so many other properties correlate with redshift in a sample such as this, limited by radio flux density, it is particularly important to ensure that the identification of multiple nuclei is not redshift-dependent. The matching of the seeing and exposure times to the redshifts of the galaxies will reduce any selection effects, but a more direct test is desirable. In Fig. 5 we show the histogram of the redshifts of the galaxies for which 0, 1 or 2 additional nuclei were found. The fraction of multiple nuclei objects is clearly fairly constant with redshift, and it is unlikely that secondary nuclei in the more distant systems are being missed. In identifying the companion galaxies there are similar problems. We adopted the simple procedure of counting as a companion any galaxy that would have been identified as a multiple nucleus if it had been located inside 19.2 kpc.

A number of interesting results are evident upon inspection of the incidence of multiple nuclei and companion objects. Overall, 10 (32 per cent) of the 31 radio galaxies have one or more secondary nuclei, including the five dumb-bell galaxies. This fraction is slightly lower than that found in the Abell sample by Schneider *et al.* (1983), but is of the same order of magnitude.

Within the radio sample, however, there are dramatic variations between the radio sources of different morphological types. Only two (14 per cent) of the radio galaxies associated with FR II sources have multiple nuclei, whereas 5 (38 per cent) of the 13 FR I sources and three out of three of the twin-tail sources have them. The single unresolved source has a single nucleus. The mean number of apparent secondary nuclei in each radio galaxy in the FR II, FR I and TT classes is 0.14, 0.53 and 1.0, respectively. Using the numbers of companion galaxies found in the 19.2–50 kpc range, it is possible to estimate how many of these so-called multiple nuclei are likely to be merely chance projections. In the 14 FR II class sources, there are a total of 16 companion galaxies, leading to the expectation that 2.7 galaxies will be found interior to 19.2 kpc, whereas in

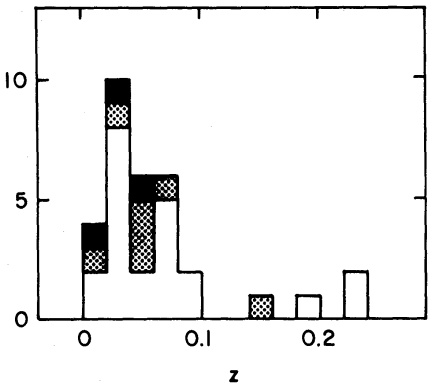

Figure 5. Incidence of multiple nuclei as a function of redshift: open boxes represent radio galaxies with no secondary nuclei, stippled those with one extra nucleus, and solid those with two or more.

Table 2. Comparison of the incidence of multiple nuclei.

		Fraction of systems that are multiple:		Mean number of secondary nuclei:	
Class	N	Observed	Corrected	Observed	Corrected
FR II	14	0.14	0.00	0.14	0.00
FR I	13	0.38	0.21	0.53	0.29
HT	3	1.00	(1.00)	1.00	(1.00)
B_{gg} < 40	8	0.12	0.00	0.12	0.00
40–80	5	0.00	0.00	0.00	0.00
80–160	5	0.60	0.43	0.60	0.43
160 < B_{gg}	4	0.75	0.55	1.00	0.74

fact only two multiple nuclei objects were found. Hence these two may well be chance projections. In the 11 FR I fields that were sufficiently distant ($z>0.015$) that the 50 kpc measurement could be made, a total of 15 companions were found, leading to a prediction that there would be three chance superpositions. Seven apparent secondary nuclei were found in five systems. Probably about half of the secondary nuclei in the FR I class are therefore likely to be genuine multiple systems. The three TT sources that had secondary nuclei are all dumb-bell galaxies and hence presumably more likely to be genuine multiple systems (see the discussion in Section 3.5). Obviously, the numbers involved in these estimates are small, but after realistically assessing the mean number of genuine multiple systems, as opposed to those consisting of simple chance projections, the percentages are of order 0, 21 and 100 per cent, respectively, for the FR II, FR I and TT sources. The corrected mean number of secondary nuclei are 0.0, 0.29 and 1.0. These figures are shown in Table 2.

There are also trends apparent in the data with the cluster richness parameter B_{gg*} discussed in the preceding section. Unfortunately, only 22 galaxies have B_{gg*} values available. Nevertheless, dividing these into four groups, those with $B_{gg*}<40$ (eight galaxies), 40–80 (five galaxies), 80–160 (five galaxies) and >160 (four galaxies) and attempting to correct for chance superposition as described above, one finds the following apparent (and corrected) percentages of multiple systems; 12 (0), 0 (0), 60 (43) and 75 (55). Multiple nuclei are clearly extremely rare for systems with low B_{gg*}. Indeed, of the 13 galaxies with measured $B_{gg*}<80$, only one has even an apparent secondary nucleus, and this is probably a chance superposition. Amongst systems with higher B_{gg*}, however, genuine multiple nuclei are probably very common, the fractions obtained here being if anything somewhat higher than those found by Schneider *et al.* (1983) in their Abell sample, although it should be noted that over half of the systems that produce these high percentages in the radio sample are the dumb-bell systems that seem to be associated predominantly with the twin-tail radio morphology.

It is interesting that the incidence of multiple nuclei increases so dramatically just at the value of $B_{gg*}\sim80$, that is associated with the poorer of the Abell clusters. Despite the fact that the numbers involved in the above estimates are small and hence susceptible to statistical fluctuations, the trends are readily apparent.

One final point concerning the incidence of nearby companions should be made. For nearly all the radio galaxies, we have counted the number of companions within 50 kpc of the centre of the radio galaxy. For the more distant ones this was also done over an area of radius 100 kpc. Given the quite large difference in the mean values of the large-scale clustering statistic B_{gg*} for the classical double FR II sources and the remaining double FR I and TT sources (37 and 134, respectively) and the difference of multiple nuclei (about 0 and 50 per cent, respectively), it is interesting, but not too surprising, that the numbers of close companions (less than 50 kpc distant)

are similar, the average numbers being 1.15 (13 FR II galaxies) and 1.31 (13 FR I and TT sources). This lack of correlation with B_{gg*} is not surprising since that statistic measures the cluster density on a very much larger scale (~1 Mpc). By 100 kpc, the difference is more apparent. The seven FR II sources that are sufficiently distant that the number of galaxies within 100 kpc could be determined from our CCD images have an average of 2.1 (ranging between 0 and 5) companions between 50 and 100 kpc, while the four FR I sources have on average 8.3 (ranging between 4 and 15).

3.5 THE DUMB-BELL GALAXIES

Reference has been made in the previous section to the association of the dumb-bell galaxies with the twin-tail (TT) radio morphology: all of the three TT sources are identified with dumb-bell galaxies. The two other dumb-bell radio galaxies have FR I structure, but in one case (0625−53) this could well be a TT source, since the radio data are of very low quality.

Four of the dumb-bell galaxies have been catalogued by Wirth, Smarr & Gallagher (1982) and have been studied on several occasions, by Zwicky & Humason (1964, 0123−01), Hoessel *et al.* (1985, 0255+05), Carter *et al.* (1981, 0428−53) and Jenner (1974, 1251−12), who have measured the differential radial velocities and, in some cases, the central velocity dispersions of the components with the aim of determining whether these systems are merging, interacting or not physically associated at all. In particular, Hoessel *et al.* (1985) have argued that 0255+05 is likely to be simply a chance projection, on the grounds that the observed velocity difference between the components of the system is larger than the central velocity dispersions of either.

Two of the five dumb-bells in the sample show convincing evidence for interaction in the sense that the isophotes are distinctly asymmetric about each nucleus. Contour plots of the surface brightness distributions in the *R*-passband of 1251−12 (z=0.015) and 0625−53 (z=0.055) are shown in Fig. 6. What is interesting is that these show distortions in a direction perpendicular to the line joining the centres of the two components. This clearly indicates interaction and suggests motion in the plane of the sky, even though 1251−12 has a differential radial velocity of over 600 km s^{-1} (Jenner 1974). The velocity difference for 0625−53 is not known. We believe that the example of 1251−12, which is clearly undergoing some form of interaction even if the

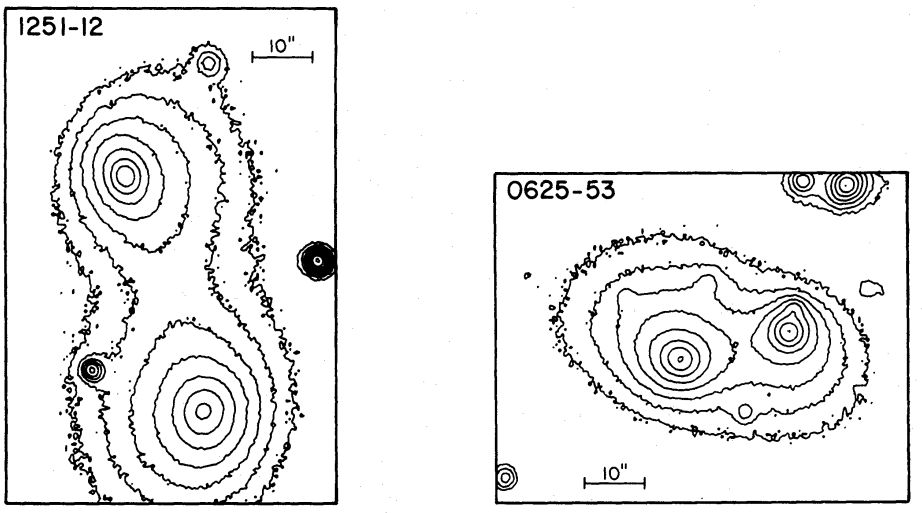

(a) (b)

Figure 6. Contour plots of the ssurface brightness distributions of the dumb-bell radio galaxies (a) 1251−12 (z=0.015) and (b) 0625−53 (z=0.055) showing the distortions induced by interactions between the components.

components are not orbiting on circular orbits, shows that it may be unwise to rely on simple velocity measurements to indicate whether a dumb-bell system is simply a projection effect.

In view of the strong association in the sample of the distinctive dumb-bell galaxies with the TT radio morphology, and of the obviously interacting cases of 1251−12 and 0625−53, we believe it unlikely that any of the dumb-bells in the sample are simple projections.

4 Discussion

The results presented in Section 3 enable us to reach some general conclusions about radio sources and about massive elliptical galaxies. In this section we explore these in turn.

What do these data tell us about the formation and properties of powerful radio sources? Most important is that they emphasize that there is a real difference between radio sources of different luminosities, in particular those above and below the break in the radio luminosity function with FR II and FR I radio structures, respectively. It has been known for some time that the large-scale radio luminosity and morphology are related to other properties, e.g. the strength of optical nuclear emission lines (Hine & Longair 1979) and the appearance and polarization properties of nuclear radio jets (e.g. Bridle & Perley 1984). Most of these properties, however, could vary over relatively short time-scales. The relation of the cluster environment (Longair & Seldner 1979: Prestage & Peacock, in preparation) and the luminosity and structure of the host galaxy (this work) to the radio luminosities and structures is important because neither the Mpc-scale environment nor the luminosity or structure of the host galaxy can change on time-scales that are comparable to the evolution of an individual radio source. At the present epoch at least, the power and structure of a radio source appear to be determined, however indirectly, by properties of the system that are fixed relatively early in the life of that system.

The twin facts that the absolute magnitudes and α parameters of the radio galaxies appear to be normal in the sense that they are similar to non-radio giant ellipticals, and that the relations between them and the cluster environment measured on scales of 1 Mpc appear to be continuous with that known for the first-ranked objects in richer (i.e. Abell) cluster samples suggests to us that it is the environment that is the important parameter in determining the radio properties. Unfortunately, despite recent improvements in technique, the cluster environment remains the least well-defined property of any given source, and is, in any case very difficult to quantify even for well-studied cluster systems. It is important to stress that the environment must be influencing not just the outer radio lobes, but also nuclear phenomena, such as the strength of optical emission lines and the properties of the radio jets.

At this time, any suggested mechanism to link the environment and the radio properties in a physical way will be speculative. Furthermore, discussion is complicated by the knowledge that both 3C 295 and Cygnus A, which are generally regarded to be prototypes of very powerful FR II radio sources, are known to lie in the upper right of the (M_V, α) diagram (Lilly *et al.* 1984) and to lie in generally richer environments than the FR II sources, properties both generally associated with FR I sources. It will clearly be important to determine the cluster environments and (M_V, α) combinations of well-defined samples of higher luminosity FR II sources (e.g. Eales 1985).

A central question in the active galaxy phenomenon is the transport of a fuel supply to the central engine. In this context it is worth emphasizing that the break in the radio luminosity function at this radio luminosity, the different cosmological evolutions of the space densities of the two populations above and below this break, and the differences in cluster environment and host galaxy structure allow the possibility that the primary transportation mode of fuel to the engine may be different in the two cases and may, of course, be different at earlier epochs.

Selection of giant elliptical galaxies by their radio emission is clearly not directly related to the number of galaxies surrounding them. While there are conceivably a number of unknown

selection effects, the radio galaxies observed in this programme are nevertheless giant ellipticals located in relatively unstudied environments, namely small clusters, which are probably not particularly compact, and are about a factor of 10 poorer than Abel clusters. That the relation between the photometric parameters and the cluster richness appears to be continuous with the richer systems suggests that the special formation process that has been inferred to produce first-ranked Abell cluster galaxies also occurred in poorer systems too. Whether this is caused by the consumption of neighbouring galaxies, fluctuations in the early universe, or some other process, remains unclear.

5 Conclusions

We have studied the optical surface brightness profiles of a sample of powerful radio galaxies and have examined the relationships of them to properties associated with the active nucleus (such as the radio luminosity and morphology and the strength and nature of optical emission lines) and the cluster environments of the galaxies. This has enabled us to reach the following conclusions:

(i) Except for the active BLRGs and BL Lac objects, powerful radio galaxies have surface brightness distributions that are similar to non-radio giant elliptical galaxies.

(ii) There are clear relations between the optical photometric parameters of a radio galaxy and the radio morphology and luminosity, strength of nuclear emission lines and cluster environment. Weaker sources with FR I morphology and $P(2.7)<10^{24.5}$ W Hz^{-1} and weak emission lines are associated with giant ellipticals that are similar to the first-ranked galaxies in Abell clusters and are located in similar environments. The more powerful FR II sources are generally identified with galaxies of somewhat lower luminosity and smaller characteristic size, and exist in poorer clusters. Sources with different radio luminosities and morphologies cannot therefore in general be different evolutionary states of a single source.

(iii) From what can be deduced about the properties of the host galaxies of the BLRGs and the BL Lac objects, they appear to be like the strong-lined NLRGs and have lower stellar luminosities than less active radio galaxies in the sample.

(iv) There is a correlation between the photometric parameters (e.g. the total optical luminosity) and the clustering statistic B_{gg^*} that measures the density of galaxies surrounding the radio galaxy at radii 1 Mpc. This correlation joins on to that present in the sample of Abell clusters, extending it by a further decade of cluster richness.

(v) The incidence of multiple nuclei is a strong function of the cluster richness: only galaxies in Richness Class 0 environments or richer have multiple nuclei. Consequently, no FR II sources have secondary nuclei. All of the three 'twin-tail' radio sources are associated with dumb-bell galaxies consisting of two components of comparable size.

(vi) Two of the dumb-bell galaxies show evidence of definite interaction in that there are isophotal distortions in a direction perpendicular to the line joining the two nuclei.

Acknowledgments

We thank Dr Bill Pence and Steve Lee for assistance in making these observations with the AAT. Data reduction and analysis was carried out on the Edinburgh STARLINK VAX using the ASPIC package and on the Princeton Observatory VAX using the UNIX VISTA package. We are indebted to Dr Tod Lauer for use of the latter, and for many very interesting discussions. Both authors were SERC/NATO Research Fellows during all or part of this work, SJL at Princeton University and RMP at Steward Observatory, and they thank their respective institutions for generous hospitality. RMP also acknowledges a SERC Studentship during which this project was started.

We thank Wendy Nakano at the Institute for Astronomy, University of Hawaii, for producing the diagrams.

References

Balick, B. & Heckman, T. M., 1982. *Ann. Rev. Astr. Astrophys.*, **20,** 431.
Bessell, M. S., 1979. *Publs astr. Soc. Pacif.*, **91,** 589.
Blair, M. & Gilmore, G., 1982. *Publs astr. Soc. Pacif.*, **94,** 742.
Bridle, A. H. & Perley, R. A., 1984. *Ann. Rev. Astr. Astrophys.*, **22,** 310.
Brazual, G., 1981. *PhD thesis,* University of California, Berkeley.
Burstein, D. & Heiles, C., 1982. *Astr. J.*, **87,** 1165.
Carter, D., Efstathiou, G., Ellis, R. S., Inglis, I. & Godwin, J., 1981. *Mon. Not. R. astr. Soc.*, **195,** 15P.
Christiansen, W. N., Frater, R. H., Watkinson, A., O'Sullivan, J. D. & Lockhart, I. A., 1977. *Mon. Not. R. astr. Soc.*, **181,** 183.
Costero, R. & Osterbrock, D. E., 1977. *Astrophys. J.*, **211,** 65.
Danziger, I. J. & Goss, W. M., 1983. *Mon. Not. R. astr. Soc.*, **202,** 703.
Danziger, I. J., Fosbury, R. A. E. & Penston, M. V., 1977. *Mon. Not. R. astr. Soc.*, **189,** 41P.
Danziger, I. J., Fosbury, R. A. E., Goss, W. M. & Ekers, R. D., 1979. *Mon. Not. R. astr. Soc.*, **188,** 415.
Danziger, I. J., Fosbury, R. A. E., Goss, W. M., Bland, J. & Boksenburg, A., 1984. *Mon. Not. R. astr. Soc.*, **208,** 589.
Eales, S. A., 1985. *PhD thesis,* University of Cambridge.
Fanaroff, B. L. & Riley, J. M., 1974. *Mon. Not. R. astr. Soc.*, **167,** 31P.
Felten, J. E., 1977. *Astr. J.*, **82,** 861.
Felten, J. E., 1985. *Comm. Astrophys.*, **XI,** 53.
Goss, W. M., Danziger, I. J., Fosbury, R. A. E. & Boksenburg, A., 1980. *Mon. Not. R. astr. Soc.*, **190,** 23P.
Graham, J. A., 982. *Publs astr. Soc. Pacif.*, **94,** 244.
Gunn, J. E. & Oke, J. B., 1975. *Astrophys. J.*, **195,** 255.
Hine, R. G. & Longair, M. S., 1979. *Mon. Not. R. astr. Soc.*, **188,** 111.
Hoessel, J. G., 1980. *Astrophys. J.*, **241,** 493.
Hoessel, J. G., Borne, K. & Schneider, D. P., 1985. *STScI Preprint Series No. 37.*
Hunstead, R. W., 1972. *Mon. Not. R. astr. Soc.*, **157,** 367.
Jenkins, C. J., Pooley, G. G. & Riley, J. M., 1977. *Mem. R. astr. Soc.*, **84,** 61.
Jenner, D. C., 1974. *Astrophys. J.*, **191,** 55.
Kirschner, R. P., Oemler, A. & Schecter, P. L., 1979. *Astr. J.*, **84,** 951.
Koski, A. T., 1978. *Astrophys. J.*, **223,** 56.
Laing, R. A., 1981. *Mon. Not. R. astr. Soc.*, **195,** 261.
Ladolt, A. U., 1983. *Astr. J.*, **88,** 439.
Large, M. I., Mills, B. Y., Little, A. G., Crawford, D. F. & Simon, J. M., 1981. *Mon. Not. R. astr. Soc.*, **194,** 693.
Leir, A. A. & van den Bergh, S., 1977. *Astrophys. J. Suppl.*, **34,** 381.
Lilly, S. J., McLean, I. S. & Longair, M. S., 1984. *Mon. Not. R. astr. Soc.*, **209,** 401.
Longair, M. S., 1966. *Mon. Not. R. astr. Soc.*, **133,** 421.
Longair, M. S. & Riley, J. M., 1979. *Mon. Not. R. astr. Soc.*, **188,** 625.
Longair, M. S. & Seldner, M., 1979. *Mon. Not. R. astr. Soc.*, **189,** 433.
Matthews, T. A., Morgan, W. W. & Schmidt, M., 1964. *Astrophys. J.*, **140,** 35.
Merritt, D., 1984, *Astrophys. J.*, **276,** 26.
Osterbrock, D. E., Koski, A. T. & Phillips, M. M., 1976. *Astrophys. J.*, **206,** 898
Peacock, J. A., 1985. *Mon. Not. R. astr. Soc.*, **217,** 601.
Pence, W., 1976. *Astrophys. J.*, **203,** 39.
Phillips, M. M. & Osterbrock, D. E., 1975. *Publs astr. Soc. Pacif.*, **87,** 949.
Sandage, A., 1973. *Astrophys. J.*, **183,** 711.
Schechter, P., 1976. *Astrophys. J.*, **203,** 297.
Schneider, D. P., Gunn, J. E. & Hoessel, J. G., 1983. *Astrophys. J.*, **268,** 476.
Smith, H. E., Spinrad, H. & Smith, E. O., 1976. *Publs astr. Soc. Pacif,* **88,** 621.
Tritton, K. P., 1972. *Mon. Not. R. astr. Soc.*, **158,** 277.
Wall, J. V. & Peacock, J. A., 1985. *Mon. Not. R. astr. Soc.*, **216,** 173.
Whiteoak, J. B., 1972. *Aust. J. Phys.*, **25,** 233.
Wirth, A., Smarr, L. & Gallaghr, J. S., 1982. *Astr. J.*, **87,** 602.
Yee, H. K. C. & Oke, J. B., 1978. *Astrophys. J.*, **226,** 753.
Zwicky, F. & Humason, M. L., 1964. *Astrophys. J.*, **139,** 267.